# Pleasing Shapes for Topological Objects


John M. Sullivan
*Technische Universität Berlin*
*sullivan@math.tu-berlin.de*
*http://www.isama.org/jms/*



Topology is the study of deformable shapes; to draw a picture of a topological object one must choose a particular geometric shape. One strategy is to minimize a geometric energy, of the type that also arises in many physical situations. The energy minimizers or optimal shapes are also often aesthetically pleasing. This article first appeared translated into Italian [Sul11].


## I. INTRODUCTION

Topology, the branch of mathematics sometimes described as "rubber-sheet geometry", is the study of those properties of shapes that don't change under continuous deformations. As an example, the classification of surfaces in space says that each closed surface is topologically a sphere with a certain number of handles. A surface with one handle is called a torus, and might be an inner tube or a donut or a coffee cup (with a handle, of course): the indentation that actually holds the coffee doesn't matter topologically. Similarly a topological sphere might not be round: it could be a cube (or indeed any convex shape) or the surface of a cup with no handle.

Since there is so much freedom to deform a topological object, it is sometimes hard to know how to draw a picture of it. We might agree that the round sphere is the nicest example of a topological sphere – indeed it is the most symmetric. It is also the solution to many different geometric optimization problems. For instance, it can be characterized by its intrinsic geometry: it is the unique surface in space with constant (positive) Gauss curvature.

More physically, we can also consider the isoperimetric problem: among surfaces in space with a fixed surface area, which one encloses the most volume? Or equivalently: among surfaces enclosing a given volume, which uses the least surface area? Surface tension causes a soap bubble, as in Figure 1, to almost instantly find the round sphere as the solution to this last problem. This answer was known to the ancient Greeks, but was first given a rigorous mathematical proof in the late 1800s.

FIG. 1: A soap bubble minimizes surface area for a given enclosed volume, and thus becomes a round sphere.

## II. BUBBLE CLUSTERS AND FOAMS

Clusters of two or more bubbles are not single smooth surfaces, but form examples of spaces that topologists call complexes: different sheets of surface joined together along curves. Again, the soap film seeks to minimize the area needed to enclose and separate the given volumes of the various bubbles. Certain basic results are known: each soap film in a cluster has constant mean curvature, and the films meet at constant angles along triple curves and at tetrahedral junctions. But bubble clusters and foams are still a source of many interesting open mathematical problems [SM96, Sul98]. For instance, it was only around the turn of this century that mathematicians proved (see [Mor01]) that the standard double bubble – made from spherical caps – beats all possible competitors as in Figure 2.

For clusters of more than two bubbles, the area-minimizer is still unknown mathematically, but clusters of three or four bubbles can again be built out of spherical pieces as in Figure 3, and these are conjectured minimizers.

Some bubble clusters have independent mathematical interest. For instance, the four-dimensional analog of the dodecahedron – known as the 120-cell or dodecaplex – can be radially projected to a three-sphere and then stereographically projected to ordinary space. The result, shown in Figure 4, is a complicated and symmetric cluster of 119 bubbles [Sul91].

A foam – as found say in shaving cream or in the kitchen sink when doing the dishes – is like a cluster of many bubbles. Mathematically it is easiest to consider infinite, triply-periodic foams that fill all of space. Lord Kelvin [Tho87] asked for the least-area foam whose cells all have equal volume. His conjectured symmetric solution remained unbeaten until more than a century after it was proposed (Figure 5): the Weaire-Phelan foam [WP94] mixes two shapes of cells and ends up with less average surface area per bubble [KS96].

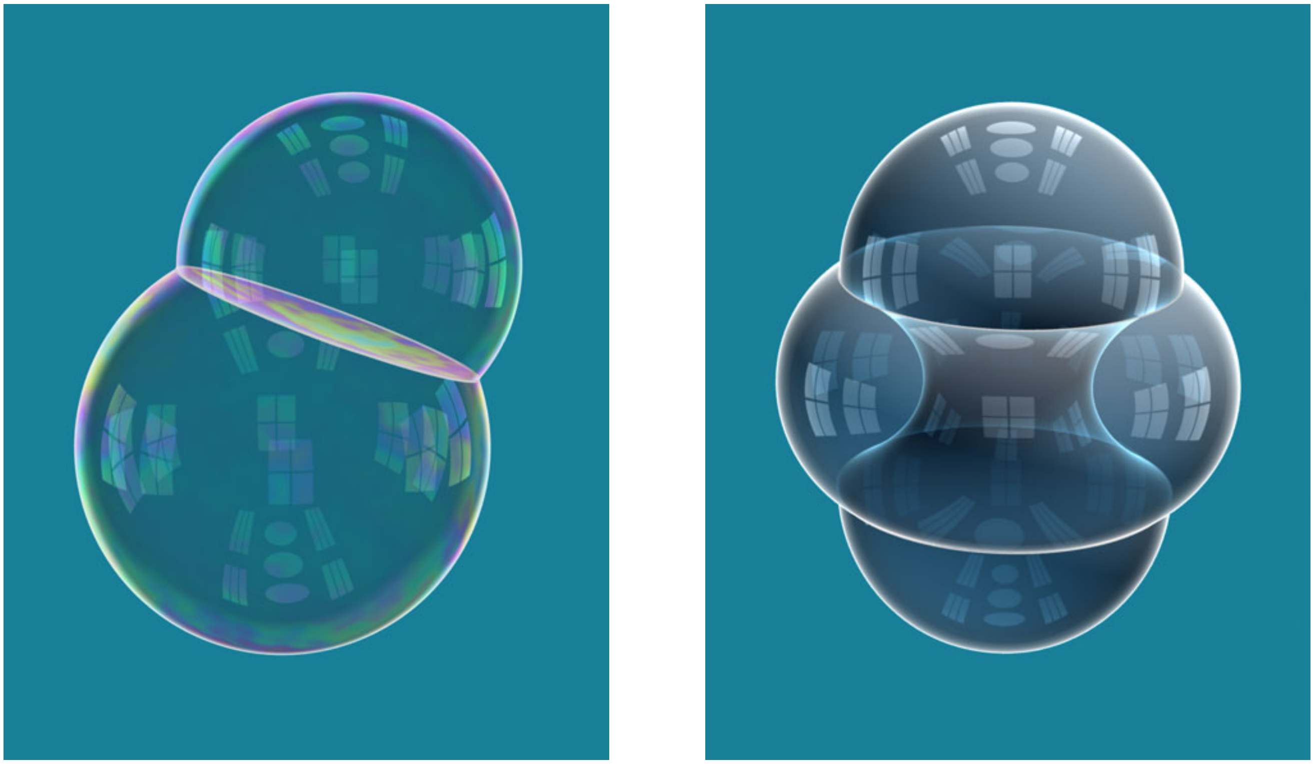

FIG. 2: A standard double bubble (left) consists of three spherical caps meeting at $120^\circ$ dihedral angles along a circle. (The inner film curves slightly away from the smaller, higher pressure bubble.) It was relatively easy for mathematicians to show that the minimizing double bubble must have rotational symmetry, but then it was hard to rule out strange configurations (right) where one bubble forms a belt around the other, or even cases where the bubbles have several disjoint components.

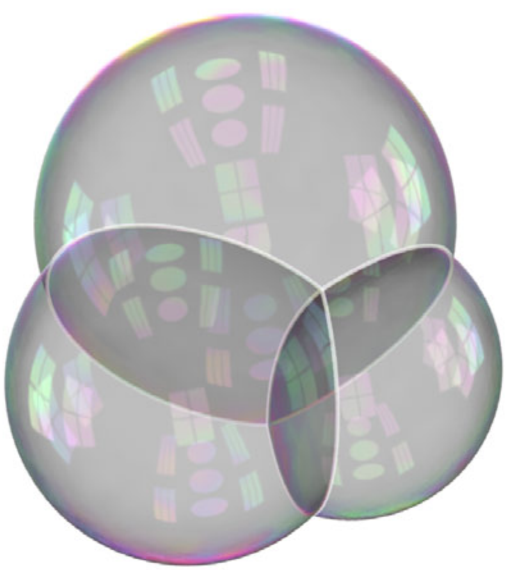

FIG. 3: The standard triple bubble is also built from pieces of round spheres meeting along circular arcs. Using Möbius transformations, we can make a version of this cluster with any desired triple of volumes. These are conjectured to be the optimal triple bubbles, but this has not yet been proven (except in 2D).

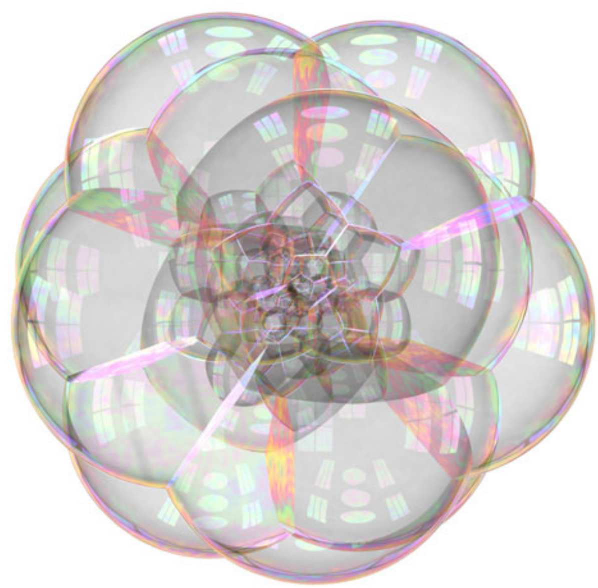

FIG. 4: This cluster of 119 bubbles is the stereographic projection of the dodecaplex or 120-cell, a regular polytope in four dimensions. One of its 120 dodecahedral cells projects to the infinite outside region. The others are arranged in seven symmetric layers around a tiny central bubble.

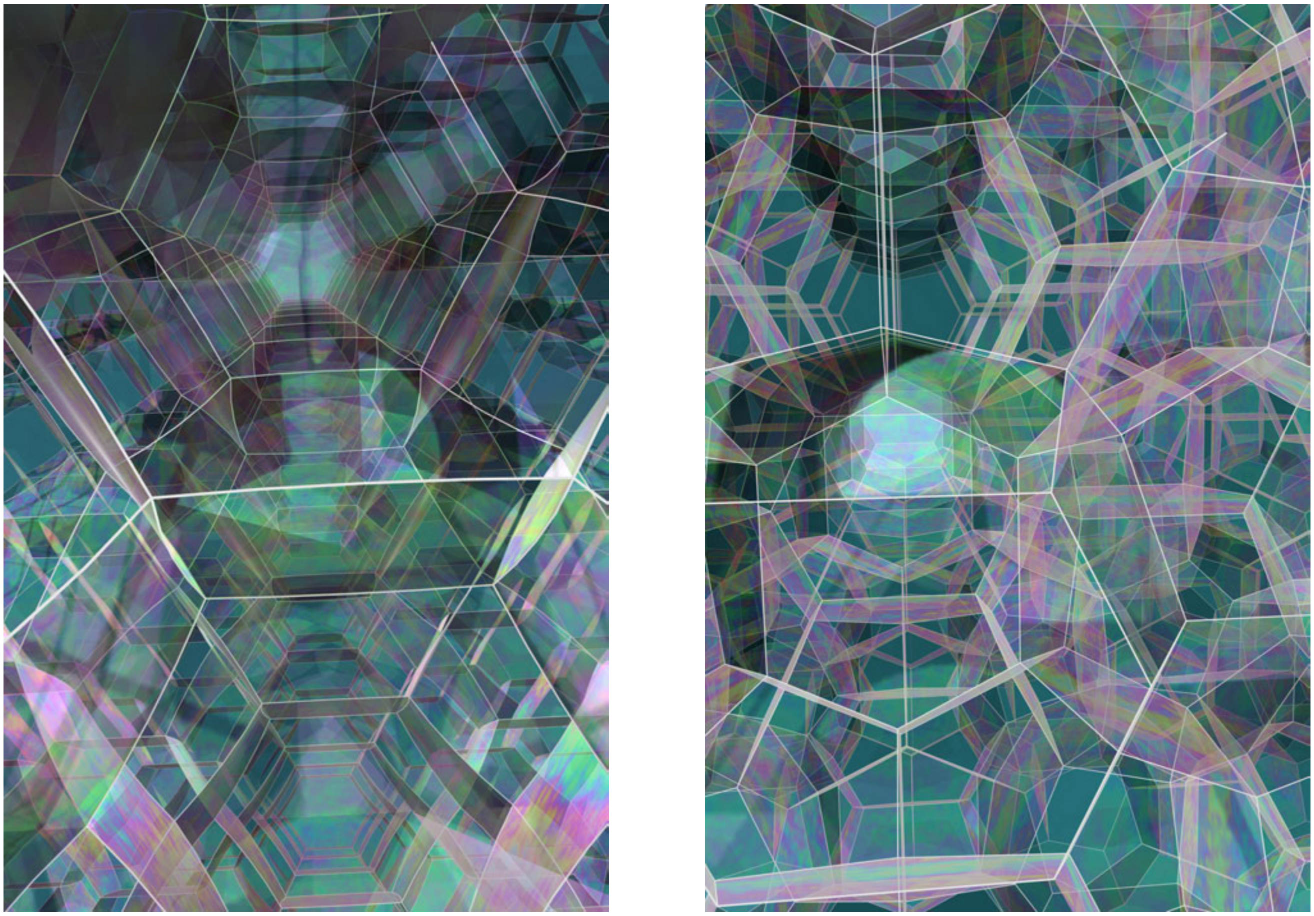

FIG. 5: The Kelvin foam (left) fills space with congruent cells, truncated octahedra tiled in a body-centered cubic lattice. The Weaire-Phelan foam (right) saves area by using two different shapes of cells, with equal volumes but different pressures. These cells fit together in a crystal pattern called A15, found in transition-metal alloys.

## III. SPHERE EVERSIONS VIA WILLMORE ENERGY

A stiff steel wire can be bent into space, but will spring back to its original straight shape. Its elastic energy in any given configuration is proportional to the integral of curvature squared. (This is analogous to Hooke's law that the energy of a spring is propotional to displacement squared.) The corresponding elastic bending energy for surfaces has several forms which are equivalent by the Gauss–Bonnet theorem: most common is the Willmore energy (see [PS87, Wil92]), the integral $W$ of mean curvature squared. Physically, many bilayer surfaces, such as biological cell membranes, seem to minimize this energy. For instance, minimizing $W$ while fixing area and enclosed volume can lead to shapes like that of a red blood cell (Figure 6).

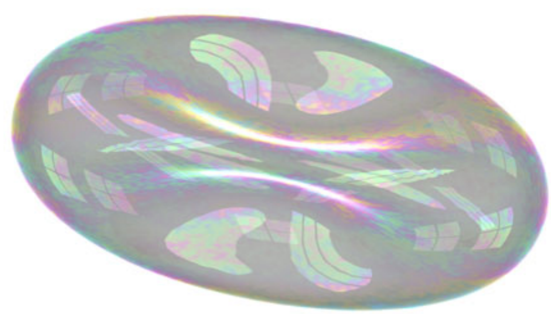

FIG. 6: This shape was obtained by minimizing the Willmore energy for fixed values of surface area and of enclosed volume. Cell membranes probably minimize this same energy, and indeed this picture is reminiscent of a red blood cell.

Mathematically, it is also interesting to consider $W$ for immersed surfaces, that is, for surfaces which are allowed to self-intersect, but which have to stay smooth, with no creases, corners or rips. The sphere in Figure 7 is immersed in a complicated way – making it hard to recognize as a sphere – but this shape is a stationary point (a saddle point) for the Willmore energy.

FIG. 7: This saddle point for the Willmore energy is obtained from a complete minimal surface with four flat ends by a Möbius transformation (inverting in a sphere). It is conjugate in a certain sense to the Morin surface of Figure 10.

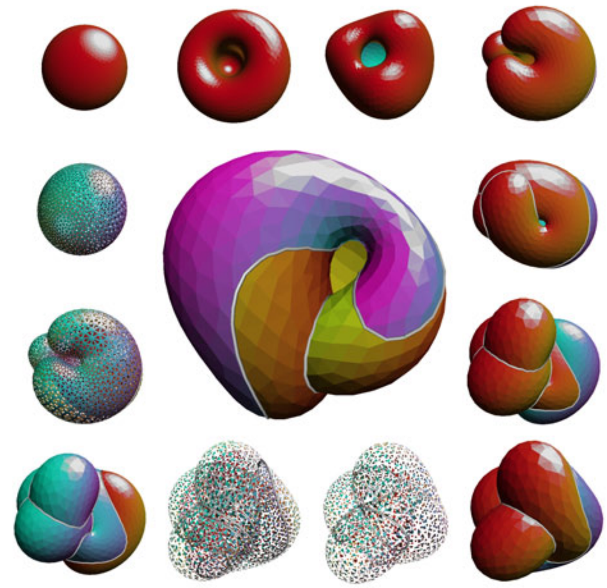

FIG. 9: The three-fold minimax eversion starts with the red sphere at the upper left and moves clockwise. The large center image and the two images below it are near the halfway stage, where we have a double cover of the Willmore Boy's surface.

FIG. 8: Tom Willmore at the mathematical research institute in Oberwolfach in the year 1998, standing next to a metal sculpture of a Boy's surface that minimizes Willmore energy, made out of ribbons of flat steel plate that have been riveted together.

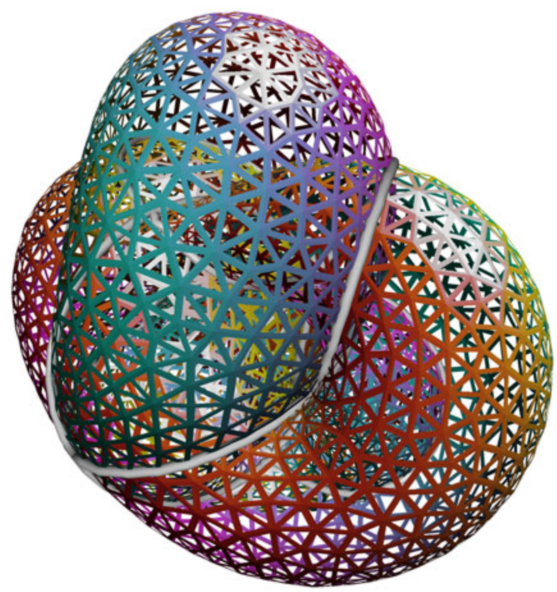

FIG. 10: A Morin surface is an immersed sphere with four lobes interchanged by rotational symmetry, two showing the inside surface (blue) and two showing the outside (red). It was described by Morin as the halfway stage of the simplest possible sphere evesion. This picture shows a Willmore-minimizing Morin surface; the white tubes highlight the self-intersection curves.

Immersed surfaces are the key to defining a sphere eversion (see [Sul99]). To turn a sphere inside out physically, we have to cut a hole in the sphere, pull the rest of the surface through the hole (as when turning a sock inside out) and then finally patch the hole. Mathematically, the interesting problem is to do this without a hole: the surface must be an entire smooth sphere at all times, but it is allowed to be immersed with self-intersections. One sheet of surface can pass through another (like a ghost through a wall) without affecting the integrity of the sphere. But again, no pinching, creasing or ripping is allowed. After Smale proved abstractly that a sphere eversion was possible, other mathematicians took years to find the first explicit eversions.

One strategy is to use a projective plane, immersed as Boy's surface, at the halfway stage. That is, in the middle of the

FIG. 11: Bernard Morin, at a conference on Art and Mathematics in Maubeuge, France in the year 2000, exploring the geometry of a Willmore-minimizing Morin surface, built on a stereolithographic printer directly from the computer data.

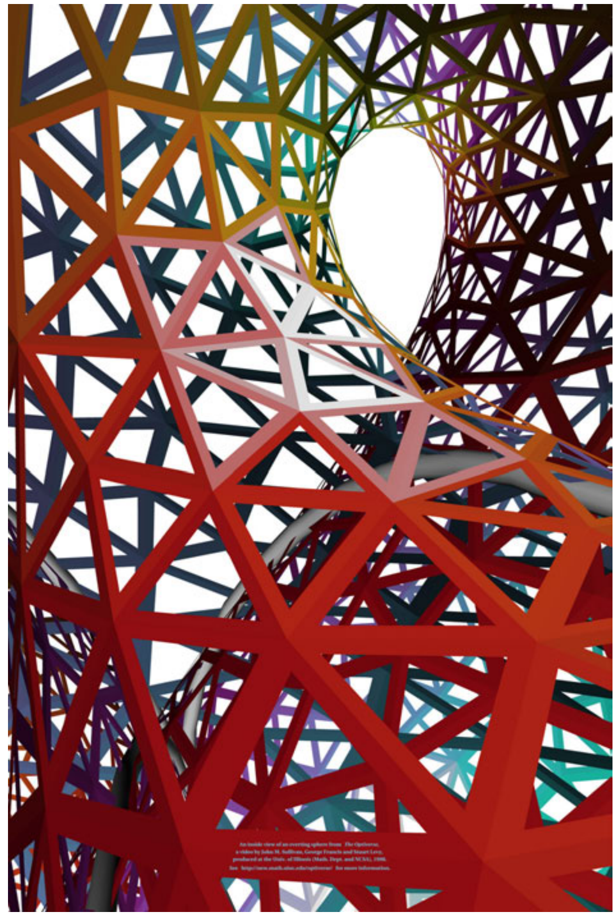

FIG. 12: We simulated the minimax eversions on the computer using polyhedral surfaces with thousands of triangular faces. To visualize the intermediate stages of an eversion, we can remove the middle of each triangle to look through the surface, and emphasize the double curves of self-intersection with white tubes.

eversion, we immerse the sphere in such a way that each pair of antipodal points maps to a single point in space: two sheets of surface always lie exactly on top of each other. To perform the eversion, we pull the sheets apart and simplify the result until it is a round sphere. The idea of the *minimax eversions* [FSK+97] is to do the simplification automatically by minimizing the bending energy $W$. This results in shapes which are more pleasantly rounded than in the topologically equivalent eversions designed earlier by hand. The halfway stage in a minimax eversion is a saddle point for $W$, for instance the Willmore-minimizing Boy's surface, which has also been depicted in a large metal sculpture (Figure 8) at the mathematical research institute in Oberwolfach, Germany [KP97].

We simulated the minimax eversions numerically, and the resulting animations were featured in our video "The Optiverse" [SFL98], premiered at the 1998 International Congress of Mathematicians in Berlin. The three-fold eversion, passing through the Willmore Boy's surface, is shown in Figure 9.

The simpler two-fold minimax eversion uses a Willmore-minimizing Morin surface (Figure 10) at the halfway stage. This immersed sphere has four lobes, and a 90-degree rotation interchanges the inside and outside. The surface is named after the blind French mathematician Bernard Morin, who described it topologically for one of the first explicit sphere eversions [FM79]. To show him what our Willmore-minimizing version of the Morin surface looks like, we presented him with a model created on a 3D-printer directly from the computer data, and he could explore it with his fingers as in Figure 11.

The two-fold minimax everion agrees topologically with Morin's eversion, and because of its relative simplicity, we can understand it well in "The Optiverse" by flying through the intermediate stages, with views like Figure 12.

With a team led by Stan Wagon, we also carved a large Morin surface (though not the Willmore version) out of snow (Figure 13) at the 2004 International Snow Sculpture Championships. The following year, we competed again, sculpting a mathematical knot.

FIG. 13: This Morin surface (left), carved out of snow at 4 meter scale, won an honorable mention for "Most Ambitious Piece" at the International Snow Sculpture Championships in Boulder, Colorado in January 2004. One year later, our team turned to knots as another source of interesting mathematical sculpture, carving a 2-fold cabling of a trefoil knot (right).

## IV. TIGHT KNOTS

Knot theory is the branch of mathematics concerned with giving a topological classification of knots – simple closed space curves – by considering which curves can be deformed into each other without crossings. Geometric knot theory looks at connections between the topological complexity of a knot and the geometric complexity of any space curve realizing that knot type. One idea, with possible relevance for physical knots tied in rope, is to consider tight knots and links, made out of rope of fixed circular cross-section, pulled tight to minimize the length of rope needed. Although some basic theory for this problem is known [CKS02], only a few tight links – where each component is a planar curve as in the Borromean rings (Figure 14) – have been described explicitly [CFK$^+$06]. This tight configuation of the Borromean rings, viewed along the axis of three-fold symmetry, has been selected as the logo (Figure 15) of the International Mathematical Union (IMU).

Some knots break their symmetry when pulled tight, or when minimizing other geometric knot energies. For instance, the $(3, 4)$-torus knot has configurations with perfect three- or four-fold symmetry. But if we minimize a certain repulsive-charge knot energy related to the Coulomb potential, this symmetry gets broken as in Figure 16. The knot then reveals itself as an interweaving of two trefoil knots.

While no tight knot of a single component is known explicitly, numerical simulations show some cases (like the Turk's head knot in Figure 17) keeping their symmetry, with pieces geometrically similar to those found in the Borromean rings.

## V. MATHEMATICAL VISUALIZATION AND ART

We have looked at a number of geometric optimization problems, and have seen how their solutions often exhibit graceful shapes. But if we want to depict them – either as three-dimensional sculptures or as two-dimensional images – there are challenges because of their complexity. Mathematically interesting curves and surfaces often have lots of hidden interior structure: the middle stages of a sphere eversion have complicated self-intersections, foams fill space with touching bubbles, and the various strands in a tight knot or link push up against each other.

Many of the figures in this article depict transparent surfaces. These are computer graphics renderings made with Pixar's RenderMan software, using the custom-made shader for soap films [AS92] that I programmed using the Fresnel laws of thin-film optics. Notably, the transparency of a soap film is much lower when viewed obliquely; this feature is missing from most simple computer graphics algorithms for transparency. Sometimes we have artificially darkened the transparent surfaces, in order to better show which sheets of the surface are in front of the others.

Often, the geometry depicted comes from numerical simulations using Brakke's Surface Evolver [Bra92]. Although this program was originally designed to minimize area, as in bubble cluster problems, the Evolver has been extended to minimize many other geometric energies, including the elastic bending energies and knot energies we have discussed. For most of the situations described here, the mathematical theory

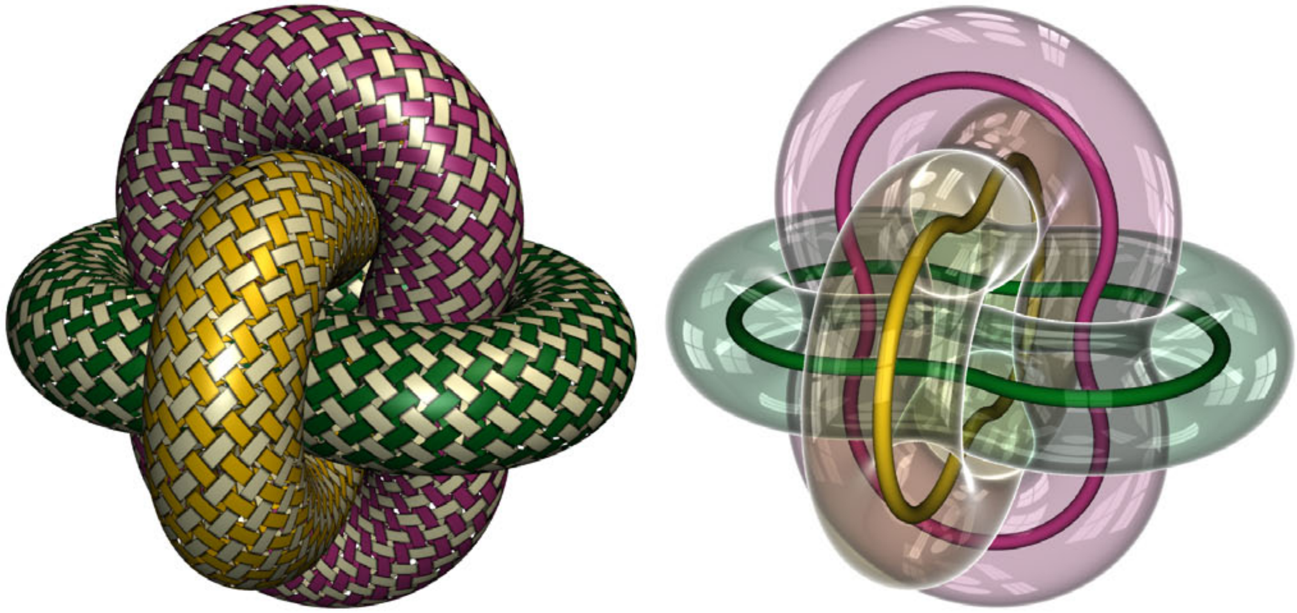

FIG. 14: The tight configuration of the Borromean rings has pyritohedral symmetry, with each component being a piecewise smooth planar curve described in part by elliptic integrals. These renderings in different styles are from the video "The Borromean Rings" [GS08a, GS08b], premiered at the 2006 International Congress of Mathematicians in Madrid.

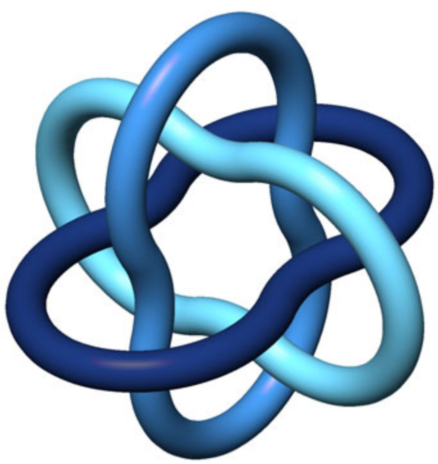

FIG. 15: The new logo of the IMU (left), chosen in an international competition, is a three-fold symmetric view of the tight Borromean rings.

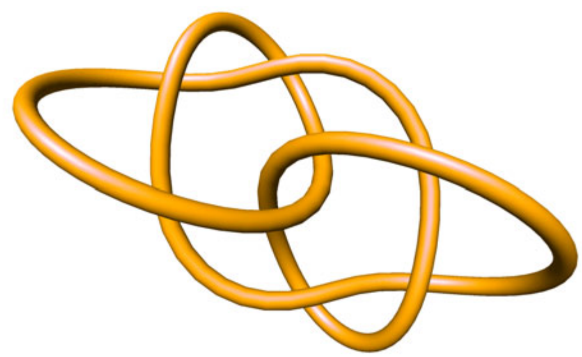

FIG. 16: The $(3,4)$-torus knot in an energy-minimizing configuration (right) breaks its symmetry and exhibits itself as two interlocked overhand knots: this has been called the "true lover's knot".

lags behind the numerical simulations, and there are interesting open problems related to proving that these pictures are accurate. The interplay between numerical simulations (with visualizations) on the one hand and rigorous proofs on the other is what allows progress on both fronts.

Optimization principles can also be used to design mathematical artwork that goes beyond pictures created primarily for visualization purposes. My mathematical sculptures *Minimal Flower 3* and *Minimal Flower 4*, shown in Figure 18, combine the ideas of minimal surfaces and knots, and were inspired by work of Brent Collins. They were first exhibited together at the Institut Herni Poincaré in Paris in 2010. The first step in creating them [Sul10] is to design a knotted boundary curve with the desired three- or four-fold symmetry and span it with a crude surface having the correct topology. Then the Evolver can be used to minimize the area of this spanning surface until it has the geometry of a soap film. Here we have to be careful to maintain the symmetry, as the deisred surfaces are unstable soap films, not least-area surfaces. The aesthetic effect is improved if we actually work in the conformal ball model of hyperbolic space, accentuating the U-shaped cross-section of the outer loops. Finally, the mathematical surface has to be given a tapered thickness to create the physical sculpture.

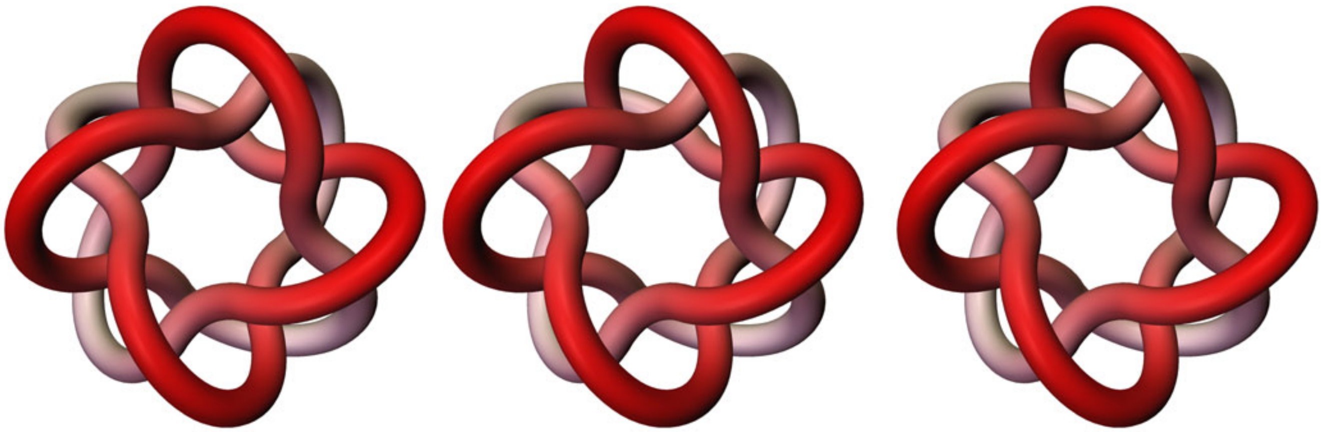

FIG. 17: A stereo view of the (presumably) tight configuration of the Turk's head knot $8_{18}$, rendered by Charles Gunn. The middle image is for the right eye: to see the stereo effect, view the left pair wall-eyed or the right pair cross-eyed.

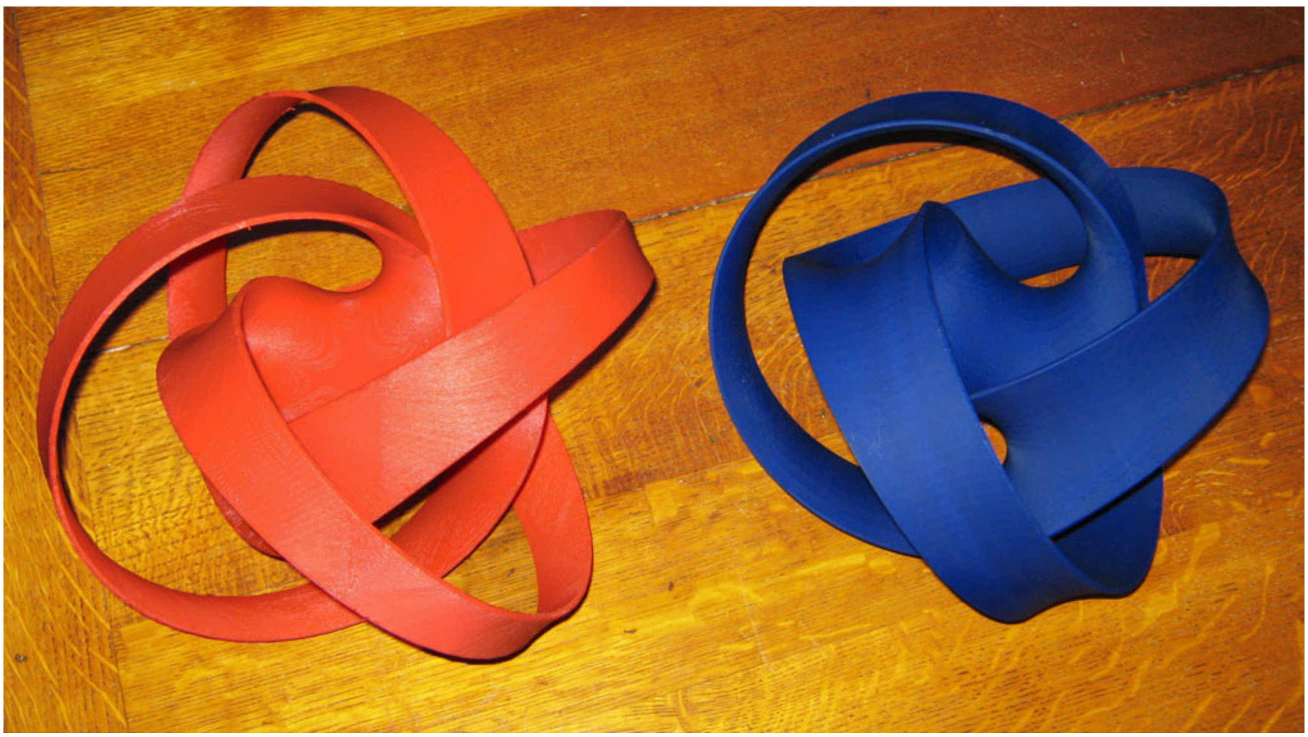

FIG. 18: The sculptures *Minimal Flower 3* and *4* depict minimal surfaces spanning knotted boundary curves. This picture was taken at the first meeting of the European Society for Mathematics and Art in Paris in July 2010.

[AS92] Frederick J. Almgren, Jr. and John M. Sullivan, *Visualization of soap bubble geometries*, Leonardo **24**:3/4 (1992), 267–271 and Color Plate C, reprinted in [Emm93].

[Bra92] Kenneth A. Brakke, *The Surface Evolver*, Experimental Mathematics **1**:2 (1992), 141–165.

[CFK+06] Jason Cantarella, Joe Fu, Rob Kusner, John M. Sullivan, and Nancy Wrinkle, *Criticality for the Gehring link problem*, Geometry and Topology **10** (2006), 2055–2115, `arXiv.org/math.DG/0402212`.

[CKS02] Jason Cantarella, Robert B. Kusner, and John M. Sullivan, *On the minimum ropelength of knots and links*, Inventiones Math. **150**:2 (2002), 257–286, `arXiv:math.GT/0103224`.

[Emm93] Michele Emmer (ed.), *The Visual mind: Art and mathematics*, MIT Press, Cambridge, Mass., 1993.

[FM79] George Francis and Bernard Morin, *Arnold Shapiro's eversion of the sphere*, Math. Intelligencer **2** (1979), 200–203.

[FSK+97] George Francis, John M. Sullivan, Rob B. Kusner, Ken A. Brakke, Chris Hartman, and Glenn Chappell, *The minimax sphere eversion*, Visualization and Mathematics (H.-C. Hege and K. Polthier, eds.), Springer Verlag, Heidelberg, 1997, pp. 3–20.

[GS08a] Charles Gunn and John M. Sullivan, *The Borromean rings: A new logo for the IMU*, MathFilm Festival 2008, Springer, 2008, 5-minute video.

[GS08b] Charles Gunn and John M. Sullivan, *The Borromean rings: A video about the new IMU logo*, Bridges Proceedings (Leeuwarden), 2008, pp. 63–70.

[KP97] Hermann Karcher and Ulrich Pinkall, *Die Boysche Fläche in Oberwolfach*, Mitteilungen der DMV **97**:1 (1997), 45–47.

[KS96] Rob Kusner and John M. Sullivan, *Comparing the Weaire-Phelan equal-volume foam to Kelvin's foam*, Forma **11**:3 (1996), 233–242, reprinted in [Wea97].

[Mor01] Frank Morgan, *Proof of the double bubble conjecture*, Amer. Math. Monthly **108**:3 (2001), 193–205.

[PS87] Ulrich Pinkall and Ivan Sterling, *Willmore surfaces*, Math. Intelligencer **9**:2 (1987), 38–43.

[SFL98] John M. Sullivan, George Francis, and Stuart Levy, *The Optiverse*, VideoMath Festival at ICM'98 (H.-C. Hege and K. Polthier, eds.), Springer Verlag, 1998, pp. 16 plus 7–minute video, `torus.math.uiuc.edu/optiverse/`.

[SM96] John M. Sullivan and Frank Morgan, editors, *Open problems in soap bubble geometry*, Int'l J. of Math. **7**:6 (1996), 833–842.

[Sul91] John M. Sullivan, *Generating and rendering four-dimensional polytopes*, The Mathematica Journal **1**:3 (1991), 76–85.

[Sul98] John M. Sullivan, *The geometry of bubbles and foams*, Foams and Emulsions (Nicolas Rivier and Jean-François Sadoc, eds.), NATO Advanced Science Institute Series E: Applied Sciences, vol. 354, Kluwer, 1998, pp. 379–402.

[Sul99] John M. Sullivan, *"The Optiverse" and other sphere eversions*, Bridges Proceedings (Winfield), 1999, pp. 265–274, `arXiv:math.GT/9905020`.

[Sul10] John M. Sullivan, *Minimal flowers*, Bridges Proceedings (Pécs), 2010, pp. 395–398.

[Sul11] John M. Sullivan, *Affascinanti forme per oggetti topologici*, Matematica e cultura 2011 (Michele Emmer, ed.), Springer Italia, 2011, pp. 145–156.

[Tho87] W. Thompson (Lord Kelvin), *On the division of space with minimum partitional area*, Philos. Mag. **24** (1887), 503–514, also published in Acta Math. **11**, 121–134, and reprinted in [Wea97].

[Wea97] Denis Weaire (ed.), *The Kelvin problem*, Taylor & Francis, 1997.

[Wil92] Thomas J. Willmore, *A survey on Willmore immersions*, Geometry and Topology of Submanifolds, IV (Leuven, 1991), World Sci. Pub., 1992, pp. 11–16.

[WP94] Denis Weaire and Robert Phelan, *A counter-example to Kelvin's conjecture on minimal surfaces*, Phil. Mag. Lett. **69**:2 (1994), 107–110, reprinted in [Wea97].